Acta Geotechnica (2009) 4:129–137
DOI 10.1007/s11440-008-0073-0

REVIEW ARTICLE

Comparison of linear and nonlinear shallow wave water equations applied to tsunami waves over the China Sea

Yingchun Liu · Yaolin Shi · David A. Yuen · Erik O. D. Sevre · Xiaoru Yuan · Hui Lin Xing

Received: 26 August 2007 / Accepted: 6 May 2008 / Published online: 31 July 2008
© Springer-Verlag 2008

Abstract This paper discusses the applications of linear and nonlinear shallow water wave equations in practical tsunami simulations. We verify which hydrodynamic theory would be most appropriate for different ocean depths. The linear and nonlinear shallow water wave equations in describing tsunami wave propagation are compared for the China Sea. There is a critical zone between 400 and 500 m depth for employing linear and nonlinear models. Furthermore, the bottom frictional term exerts a noticeable influence on the propagation of the nonlinear waves in shallow water. We also apply different models based on these characteristics for forecasting potential seismogenic tsunamis along the Chinese coast. Our results indicate that tsunami waves can be modeled with linear theory with enough accuracy in South China Sea, but the nonlinear terms should not be neglected in the eastern China Sea region.

Keywords China Sea · Nonlinear shallow-water equations · Numerical computation · Tsunami waves

Y. Liu
South China Sea Institute of Oceanology,
Chinese Academy of Sciences, Guangzhou, China

Y. Shi
Graduate University of Chinese Academy of Sciences,
Beijing, China
e-mail: shiyl@gucas.ac.cn

D. A. Yuen
Department of Geology and Geophysics,
University of Minnesota, Minneapolis, USA

Y. Liu (✉) · D. A. Yuen · E. O. D. Sevre
Minnesota Supercomputing Institute,
University of Minnesota, Minneapolis, USA
e-mail: spring.yingch@gmail.com

H. L. Xing
ESSCC, University of Queensland,
Brisbane, Australia

X. Yuan
Key Lab of Machine Perception and School of EECS,
Peking University, Beijing, China

1 Introduction

Models of shallow water wave equations are widely used in tsunami simulations [1, 4, 5]. The shallow water wave equations describe the evolution of incompressible flow, neglecting density change along the depth. Shallow water wave equations are applicable to cases where the horizontal scale of the flow is much bigger than the depth of the fluid. Therefore, tsunami waves can be described by shallow water models. A simple yet practical numerical model describing the propagation of tsunamis is given by the linear shallow water wave equations. They are the simplest form of the equations of tsunami propagation, which does not contain the nonlinear convective terms. In recent years, many destructive tsunamis have served as a reminder that it is important to develop a well-coordinated strategy for issuing tsunami warnings. To make a timely prediction of tsunami wave propagation in the open deep oceans, numerical simulations based on linear theory with the linear shallow-water equations are desirable because they involve a short amount of computation. In the presence of sharply varying bathymetry of the China Sea, it is important to carry out a detailed comparison between the linear and nonlinear theory for different values of bottom friction and ocean depths. Tsunami simulations are often carried out using linear shallow water modeling because it is

computationally faster and easier to perform without the need to specify the seabed boundary condition. In this paper, we find the boundary condition specification to be very important for obtaining accurate results on the coastal area in tsunami propagation process. In addition, the difference in computing times for linear and nonlinear models is very substantial. The nonlinear model typically would take about four to five times computing time than the linear model for high-fidelity simulations.

China Sea region consists of two major sea areas: South China Sea, and eastern China Sea, with the latter part composed of the East Sea, Yellow Sea, and Bohai Sea. There exist tsunami records going back to more than 2,000 years since DC 47 [16]. The coastal areas of China that were influenced by tsunami hazard are mainly concentrated in three regions: Hong Kong costal area, Jiangsu and Zhejiang coastal area, and south-western and north-eastern of Taiwan island. Chinese Sea is located at the interacting region between the Eurasian Plate and the Philippine Sea Plate. The interaction is the most active among the global subduction zones. The historical seismic data distribution of East Asia plate area depicts earthquakes mainly concentrated in the Ryukyu island arc, Taiwan, and the Manila trench. On the other hand, earthquakes rarely occur in the China Sea territory, not to mention large earthquake series in this same area. This shows that subduction zones between the Philippines Sea plate and the Eurasian Plate represent stress concentration regions of East Asian plate [21]. The Okinawa trough and Manila trench are the largest seismogenic tsunami source that could seriously impact the Chinese coastal area [12]. In our study, we forecast the potential tsunami hazard

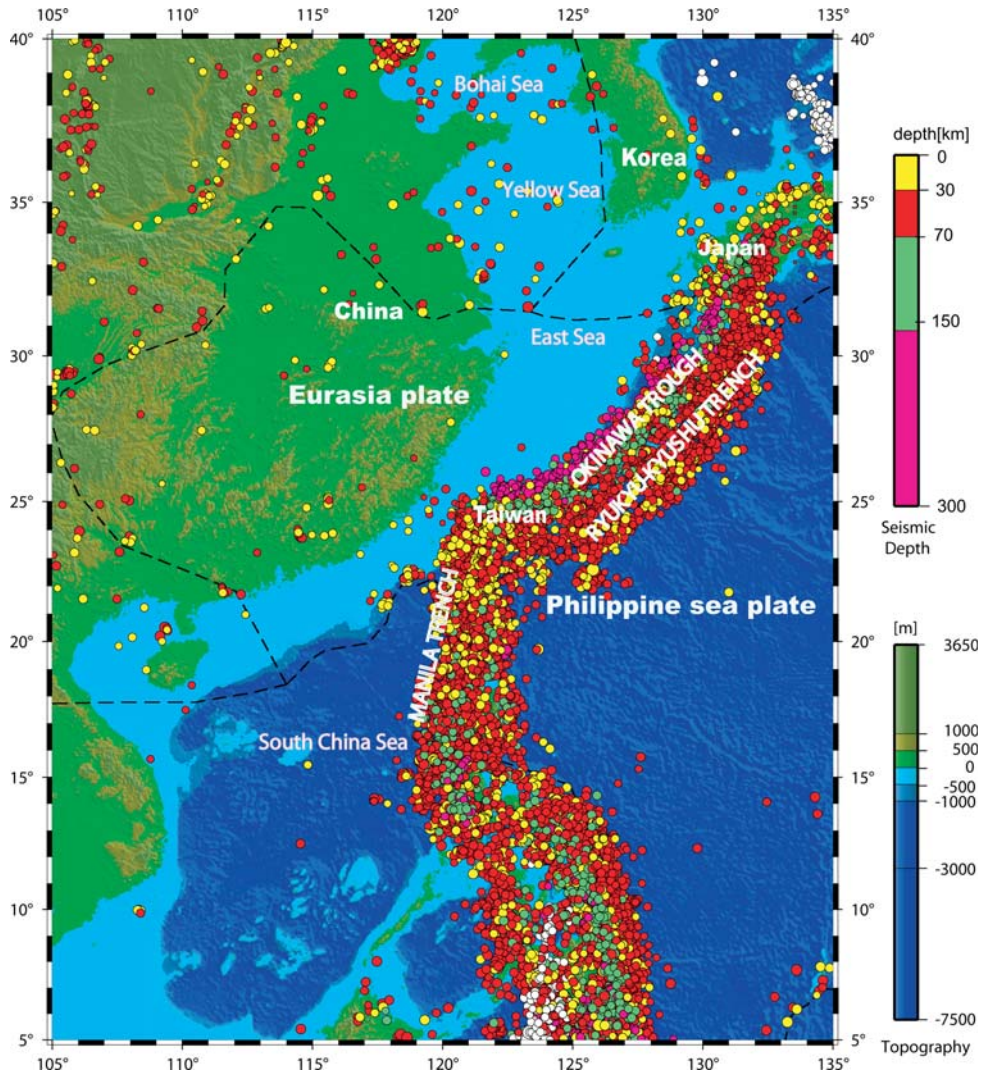

Fig. 1 Topographic and tectonic map of China Sea region and its adjacent regions. Historical earthquakes distribution with the epicenter also is shown. Database comes from NEIC (1976–2007) (http://www.ngdc.noaa.gov/seg/hazard/tsu_db.shtml)

along the Chinese coast by combining the seismic activities study and tsunami simulations [11, 12]. The bathymetries of two ocean regions are extremely different. As illustrated in Fig. 1, the average depth of South China Sea is more than 1,000 m. However, the depth of East China Sea is around 300 m. Because of a rather unique bathymetry of China Sea, we employ the linear and nonlinear shallow water wave equations for South China Sea region and East China Sea region, respectively.

2 Comparison of linear and nonlinear shallow water models

The South China Sea (SCS) (Fig. 2), lies in the middle of the Eurasia Plate, Philippine Sea Plate, and Australia Plate. It is the largest marginal sea along the continental margin of East Asia [13]. It is an ideal setting for testing the linear and nonlinear properties of tsunami waves because of its great range in seafloor depth, from 7,000 to around 10 m. We have pooled together various studies by including the geology, geophysics, seismology, and geodesy [11] in South China Sea region. They all show that subduction zones between the Philippine Sea plate and the Eurasian Plate are regions of strong stress concentration in the East Asian plate. The Manila trench is probably the largest seismogenic tsunami source that could seriously impact coastal area of China bordering South China Sea [11].

Seismogenic tsunami generation is a very complicated dynamical problem. Certain factors affecting tsunami sources include the duration period of earthquake rupture, geometric shape of rupture, bottom topography near the epicenter of earthquake, seismic focal mechanism, and rock physical properties [3]. Ward [18] studied tsunamis as long-period, free oscillations of a self-gravitating earth, with an outer layer of water representing a constant depth ocean. The tsunami displacement field can be constructed by summing the normal modes of the spherical harmonics. Comer and Robert [2] regarded the tsunami source excitation in the flat Earth by a point source. He emphasized that a source problem in the flat Earth differs substantially from the corresponding problem for the spherical Earth. Yamashita and Sato [20], using the fully coupled ocean–solid Earth model, analyzed the influence

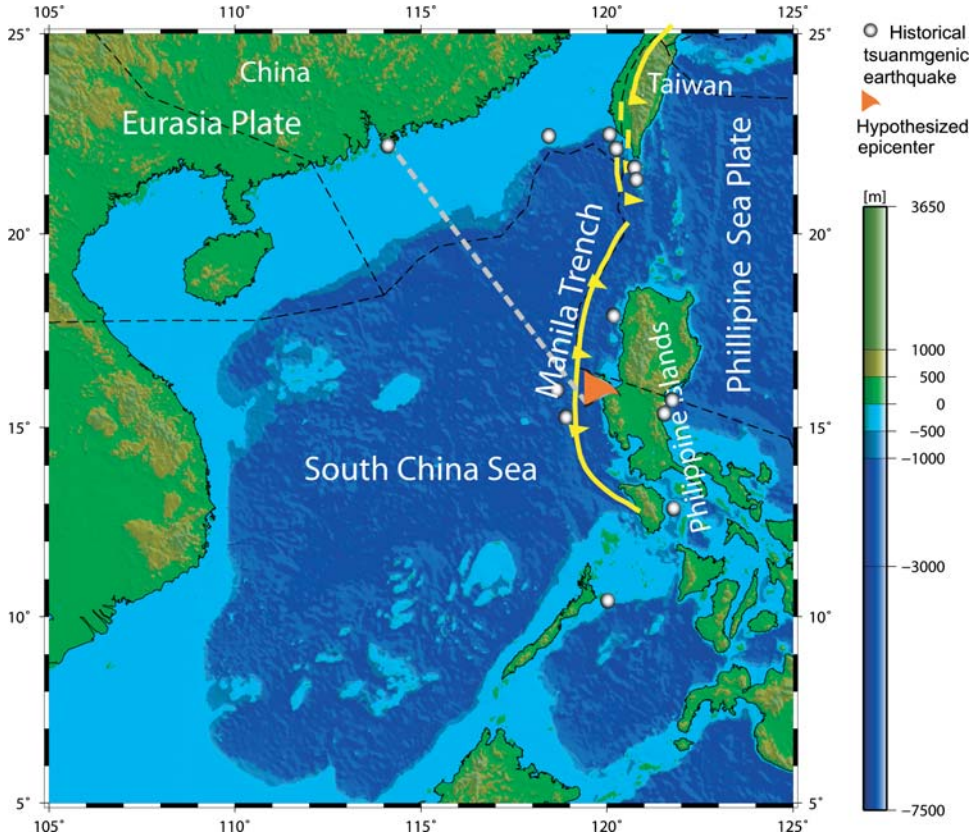

Fig. 2 Topographic and tectonic map of South China Sea and its adjacent region. *Grey ball* represents the historical seismic tsunamis catalog from NGDC/NOAA. The marked hypothesized epicenter is used in Figs. 3, 4, and 6. A total of 31 receivers are placed on a straight line from epicenter to Hong Kong

of the parameters of seismic focal mechanism, such as dip angle, fault length, focal depth, and the rise time of the source time function on tsunami. They took wave forms of tsunami as long period gravity wave and Rayleigh waves.

We assume one tsunami source model as a function which depends on time, the geometry of bottom topography, and other factors. The influence of different tsunami sources with the assumed model or normal elastic bottom displacement on wave propagation is that wave dispersion can be significantly influenced in nonlinear shallow water models for amplitude estimation in tsunami propagation with wave train generated in time-dependent rupture model [8, 10]. In fact, a more realistic time-dependent source function can be used. For a seismogenic tsunami, the time duration for the earthquake, in the order of minutes, could be neglected when compared with the total time of tsunami propagation, which is from a few hours to more than 10 h. Therefore, the model of tsunamogenic coseismic earthquake can be treated as an elastic model. Many previous studies have used an elastic dislocation model constrained by the seismic focal mechanism for an earthquake excitation tsunamic source.

In our models, the initial condition of the linear shallow water equation is computed according to Okada's work [14], which is the numerical result of the elastic seabed displacement of the coseismic deformation. A rectangular 2D fault embedded within an elastic half-space model was adopted to represent major faults of the seismic origin for calculating the earthquake induced tsunamis. The advantage of the Okada model in tsunami modeling is that it can provide fast computing which is very important for early tsunami warning. We analyze by embodying the seismic, geological and geophysical background, and determining the location of potential tsunamogenic earthquakes. We have chosen the SCS region to investigate the differences between the linear and nonlinear models. The earthquake magnitude is set to be 8.0. In the seismic models, source parameters (rupture length L, width W, and the average slip D) are derived from theoretical and empirical relationships [19] that have been widely applied. The fault dips and strikes from the composite fault plane solutions come from the average dip of the fault segments according to the Harvard catalog (http://www.globalcmt.org/CMTsearch.html). Since the shallow water region in South China Sea is relatively narrow, the linear model describing the tsunami wave propagation for this area is considered first. Here, the bottom friction is ignored. We apply the linear shallow water theory for a Cartesian system. Due to the low latitude of the South China Sea, the Coriolis effect can be safely neglected. The following linear shallow-water Eq. (1) are employed.

$$\begin{aligned}
&\frac{\partial z}{\partial t}+\frac{\partial M}{\partial x}+\frac{\partial N}{\partial y}=0\\
&\frac{\partial M}{\partial t}+gD\frac{\partial z}{\partial x}=0\\
&\frac{\partial N}{\partial t}+gD\frac{\partial z}{\partial y}=0
\end{aligned} \tag{1}$$

Due to the existence of the shallow water region in South China Sea, as a comparison, we also employ the nonlinear shallow-water model. Here, we include the effect of the friction coefficient on the wave height. the nonlinear equations (2) are given by:

$$\begin{aligned}
&\frac{\partial z}{\partial t}+\frac{\partial M}{\partial x}+\frac{\partial N}{\partial y}=0\\
&\frac{\partial M}{\partial t}+\frac{\partial}{\partial x}\left(\frac{M^2}{D}\right)+\frac{\partial}{\partial y}\left(\frac{MN}{D}\right)+gD\frac{\partial z}{\partial x}+\frac{\tau_x}{\rho}=0\\
&\frac{\partial N}{\partial t}+\frac{\partial}{\partial x}\left(\frac{MN}{D}\right)+\frac{\partial}{\partial y}\left(\frac{N^2}{D}\right)+gD\frac{\partial z}{\partial y}+\frac{\tau_y}{\rho}=0
\end{aligned} \tag{2}$$

In both models z is the instantaneous water height, t is time, x and y are the horizontal coordinates, M and N are the discharge fluxes in the horizontal plane along x and y coordinates, $h(x,y)$ is the undisturbed basin depth, $D = h(x, y) + z$ is the total water depth, ρ is density of water, g is gravity acceleration and f is bottom friction coefficient. τ_x and τ_y are the tangential shear stresses in x and y direction. In the nonlinear model, the effect of friction on tsunami wave propagation is included. The bottom friction is generally expressed as follows [5]:

$$\begin{aligned}
&\frac{\tau_x}{\rho}=\frac{1}{2g}\frac{f}{D^2}M\sqrt{M^2+N^2}\\
&\frac{\tau_y}{\rho}=\frac{1}{2g}\frac{f}{D^2}N\sqrt{M^2+N^2}
\end{aligned} \tag{3}$$

We will not get into a detailed discussion of function f here. Rather, we will use the Manning roughness n, which is familiar to civil engineers. The friction coefficient f and Manning's roughness n are related by $n=\sqrt{fD^{\frac{1}{3}}/2g}$. This relationship holds true when the value of total depth D is small. Under this condition, f becomes rather large and makes n nearly a constant value. Thus, the bottom friction terms can be expressed by

$$\begin{aligned}
&\frac{\tau_x}{\rho}=\frac{n^2}{D^{7/3}}M\sqrt{M^2+N^2}\\
&\frac{\tau_y}{\rho}=\frac{n^2}{D^{7/3}}N\sqrt{M^2+N^2}
\end{aligned} \tag{4}$$

Throughout this model, the expression for bottom friction given in Eq. 4 is used. The parameter depends the condition of the bottom surface. We will make a detailed comparison for different Manning constants in the nonlinear model.

In our simulations we have employed the linear tsunami propagation model Tunami-N1, and nonlinear model Tunami-N2, developed in Tohoku University (Japan) and provided through the Tsunami Inundation Modeling Exchange (TIME) program [5]. This tsunami code ensures the numerical stability of linear and nonlinear shallow water wave equations with centered spatial and leapfrog time difference [5]. We use the open boundaries conditions in these models which permits free outward passage of the wave at the open sea boundaries. The computational stability depends on the relationship between the time step and spatial grid-size. Furthermore, the computational stability is also constrained by the physical process in the models. Here, the model physics must satisfy the CFL criterion, that is $\Delta s/\Delta t > |\sqrt{gh}|$, where Δs is spatial grid size, Δt is time step, g is acceleration of gravity, and h is water depth. The bathymetry of the South China Sea was obtained from the Smith and Sandwell global seafloor topography (Etopo2) with grid resolution of near 3.7 km. The total number of grid points in the computational domain is 361,201, which is 601 × 601 points. The time step, Δt, in both models is selected to be 1.0 s to satisfy the temporal stability condition. In our simulation, since the bottom friction coefficient is larger than zero, we have $D = h + z > 0$, where D is total water depth, h is water depth, and z is wave height. This means that shallow water wave equations can maintain computational stability only within a computational domain filled with fluid [17]. Since the wave height of tsunami wave is only a few meters in the propagation process, we have set the smallest computational depth as the order of 10 m along coastal area in both linear and nonlinear models. This way, all of the computation domain satisfies this condition.

As mentioned in the introduction, there exists a significant difference in the computing time and computational circumstance between the two models. Linear models can run on a single PC, whereas nonlinear models need more computing power. We performed linear and nonlinear modeling using our group computer with four Central Processing Units of an Opteron-based system. The runtime for the nonlinear model is 180 min, or 4.5 times longer than the linear models, which is 40 min for 6.0 h wave propagation computing.

To validate the wave propagation process in linear and nonlinear models, we place 31 receivers along the straight line between the epicenter in the Philippines and Hong Kong, as shown in Fig. 2. This hypothetical tsunami earthquake occurs southwest of the Philippines (14.5°N, 119.2°E), with a magnitude of 8.0. For comparison between the linear and nonlinear models, we perform our first simulations under the condition of $n = 0.025$, recommended by Imamura, as the bottom friction coefficient in this situation [5]. The value $n = 0.025$ is suitable for the natural channels in good

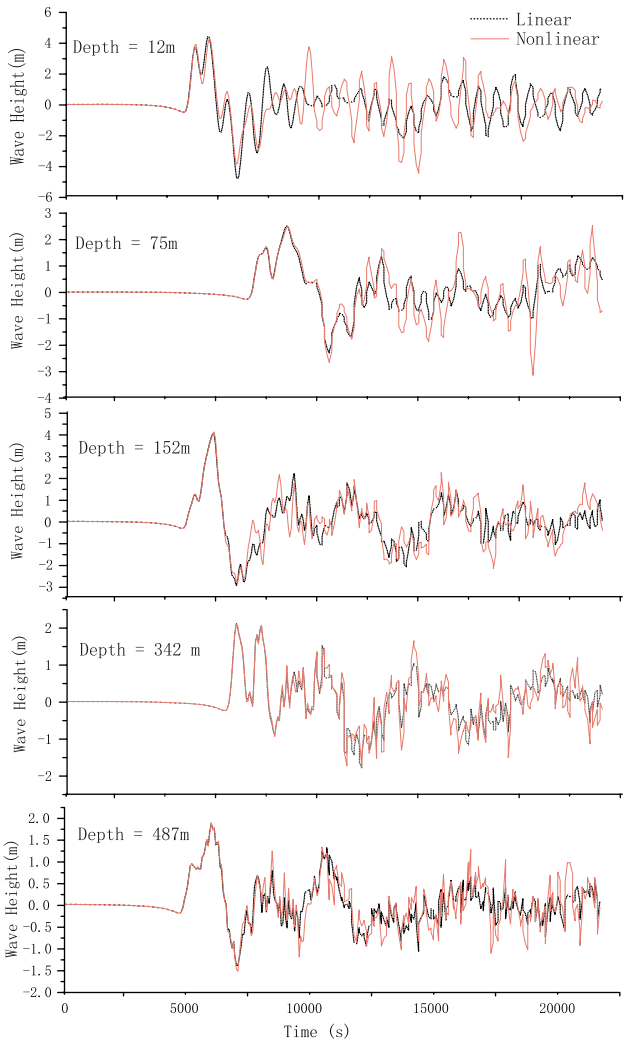

Fig. 3 Comparison of water heights in time-series with linear and nonlinear models for various water depths in South China Sea region. These waves are taken at the receivers located on a straight line between the epicenter (marked in Fig. 2) and Hong Kong

condition which is valid for the South China Sea regions. We illustrate the comparison of water heights in time histories with linear and nonlinear models in various water depths, from 12 to 3,792 m. (Figs. 3, 4). These waves are taken at the receivers located on a straight line between the epicenter (marked in Fig. 2) and Hong Kong. Because the friction force is $1/D$ in Eq. 4, when the water depth is very deep, the friction influence can be neglected. In other words, the deeper the water level, the less the frictional influence present. On the other hand, close to the shallow water region, the seabed friction tends to dominate. The comparison figures show that there is one critical zone between 400 and 500 m depth. With the ratio of wave height to water depth smaller than 0.01, wave propagation can be modeled by the linear theory with reasonable accuracy. Otherwise, the nonlinear model is necessary for making accurate

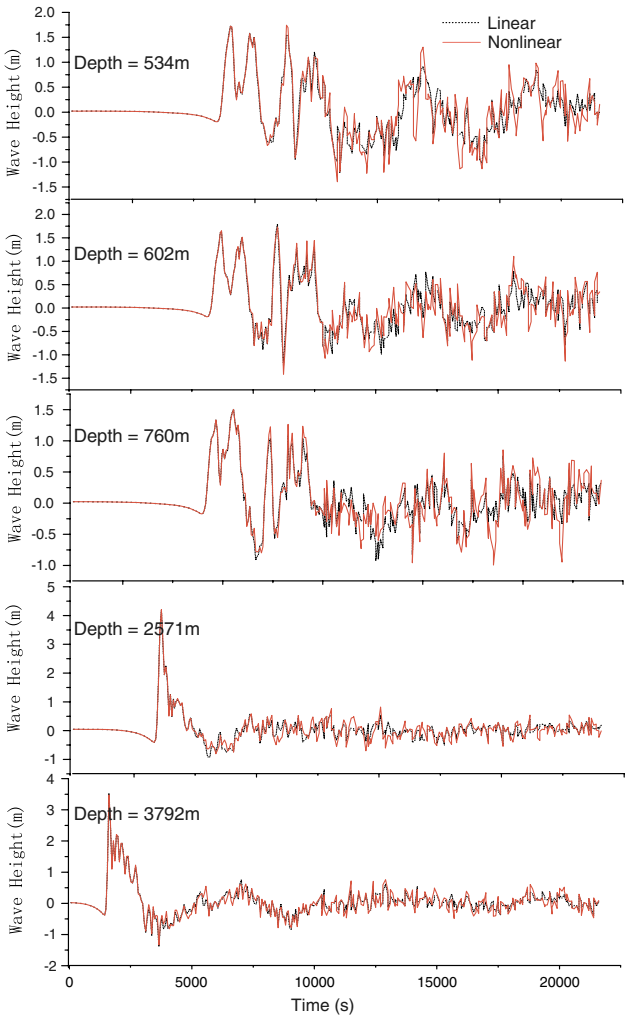

Fig. 4 Comparison of water heights in time-series with linear and nonlinear models for various water depths in South China Sea region. These waves are taken at the receivers located on a straight line between the epicenter (marked in Fig. 2) and Hong Kong

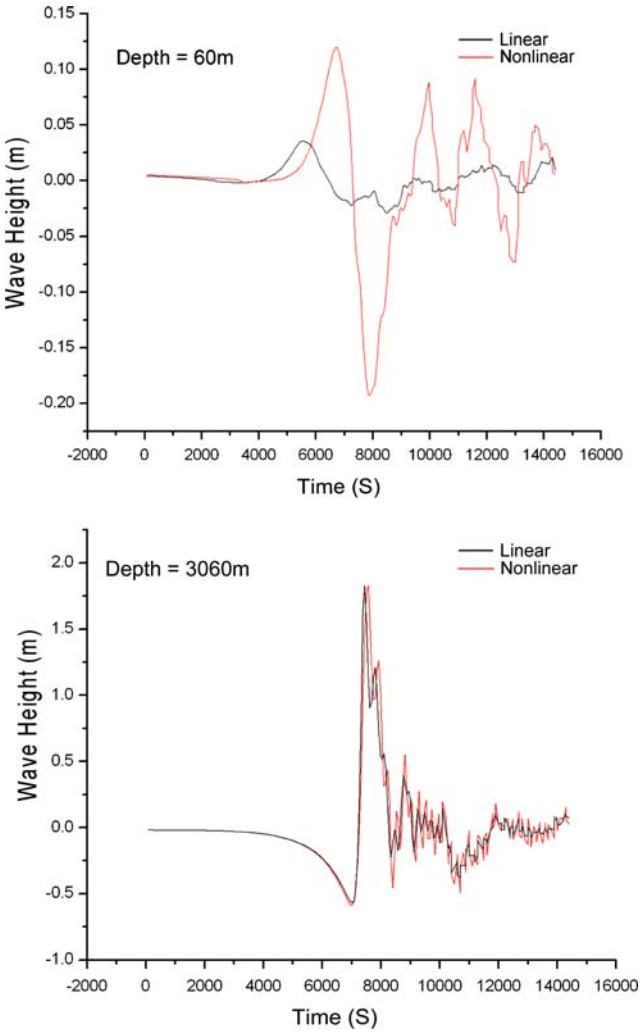

Fig. 5 Comparison of water heights in time-series with linear and nonlinear models for various water depths in eastern China Sea region. (Only the results of the first 4.1 h are plotted to avoid visual congestion). The epicenter is located in Okinawa trough (Fig. 1)

assessments. If water depth is lower than the critical range, the absolute value of wave height for nonlinear models is bigger than that of the linear models with the convection terms dominating in nonlinear shallow water wave equations. Above this depth, both the linear and nonlinear models generate similar wave shapes and wave magnitudes.

In order to distinguish the two models, we have also employed the same codes of SCS to compare tsunami wave in eastern China Sea region (Fig. 7). The resolution grid of eastern China Sea region is higher than that in South China Sea area to eliminate wave dispersion in nonlinear models with Etopo1 topographical data. Grids number is 1201×1201, or 1,442,401. The nonlinear model completed in about 10 h; in contrast, the linear models finished in about 2 h. In this area, the ratio of running time between the nonlinear and linear models is around 4–5. We also set receivers along one straight from epicenter to coast in different water depth. The hypothetic seismic epicenter is set in Okinawa trough. Here, we only show two tsunami wave curves: one is on the oceanic depth of 60 m, the other is on depth of 3,060 m (Fig. 5). The temporal wave height curves in two regions present that the features of first arriving waveforms in linear and nonlinear models are influenced by the topographical condition of entire computational domain. As shown in Figs. 3 and 4, the first arriving waveforms of linear and nonlinear models are similar in South China Sea region. Because the average depth of South China is around 1,000 m and the area covering with water depth shallower than 500 m is very narrow. The bottom friction influences less in nonlinear models in the entire wave propagation process. On the other hand, the first arriving waveforms of linear and nonlinear models (Fig. 5) are very different both in arriving times and wave heights in eastern China Sea region. Most water depth of eastern Chinese area is less than

300 m, except in Okinawa trough, it is deeper than 1,500 m. The sea-bottom friction and convection terms in nonlinear models act as the main factor that make the first arriving wave large different in the linear and nonlinear models with shallow water depth in the eastern China Sea region. The bottom friction makes the first arriving wave of nonlinear model lag that of linear model in shallow ocean part (The ocean depth is 60 m). The convection term induces the wave height of first wave of nonlinear models is higher than that of linear models. At the same time, the waveforms of two models in deep ocean part (The ocean depth is 3,060 m) reconfirm the results of linear and nonlinear models are similar in South China Sea region. According to computational results of linear and nonlinear models in two areas, we must take care of nonlinear terms in shallow oceanic area in tsunami simulation, such as eastern China Sea region. On the other hand, we can apply linear theory to a good accuracy for the South China Sea.

Now, we consider the effects of the Manning values on the prediction of tsunami wave heights with nonlinear modeling in SCS region. Three Manning values, 0.025, 0.060, and 0.125, for various coastal conditions as suggested by Imamura [5], are used. $n = 0.025$ is for the natural channels in good condition, $n = 0.060$ is for very poor natural channels, and $n = 0.125$ is a hypothetical number for better modeling effects of sea bottom friction on the wave height. Here, we only consider the water regions with depth lower than 500 m, with tsunamis having dominating nonlinear properties. In Fig. 6, the effects of three different Manning roughness on the wave have been compared for points at depths of 12, 152, 255, 342, and 487 m, respectively, that also located on at the straight line from the hypothetical epicenter to Hong Kong (Fig. 2). The figure shows the wave height of the tsunami to be very sensitive to the friction term. With different Manning roughness, the effect of the frictional term on the initial waves is marginal. This is because that the energy of the initial waves is very strong and not sensitive at all to the Manning roughness. However, for the subsequent waves developed, with a much lower energy after over 8,000 s of propagation, the frictional term exerts a much larger effect on the wave height. In shallow water regions (e.g., 12–75 m), the dynamical effect from the bottom friction is strong.

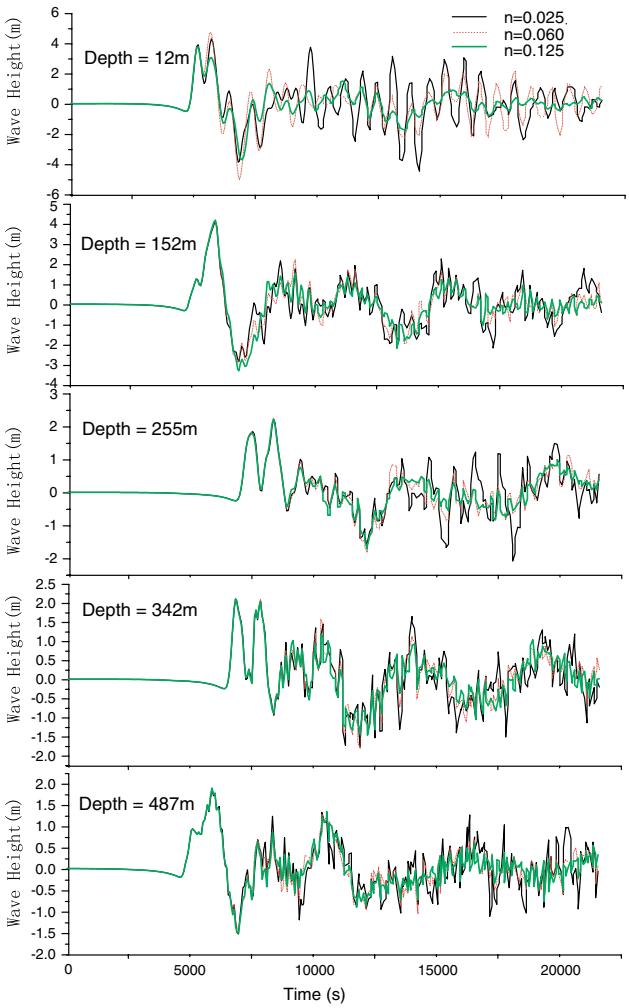

Fig. 6 Comparison of water height in time histories with different Manning roughness ($n = 0.025$, 0.060, and 0.125) for various water depths. These stations lie along the same line as in Fig. 2 but at the different depths

3 Probabilities of potential tsunami hazard along China Sea coast

The characteristics of Chinese tsunami hazard have a long cycle with 1,000-year-period. We devise a new method, called the Probabilistic Forecast of Tsunami Hazards, in order to determine potential tsunami hazard probability distribution along Chinese coast [11]. In this method, we first locate the potential seismic zone by analyzing the detail of the geological and geophysical background, the seismic activities by Gutenberg-Richter relationship [7, 15]. Then, we simulate the tsunamis excited by potential earthquakes and we compute the heights of waves hit the coast are computed. Finally, Probabilistic Forecast of Tsunami Hazards is computed based on Probabilistic Forecast of Seismic Hazards [11], and potential tsunami hazard distribution along Chinese coast is mapped. Historical seismogenic tsunami data can provide the most reliable basis for the study of tsunami hazard. Unfortunately, in China, there are few scientific papers that deal with the analysis of tsunamis. The reliable numerical tsunami simulation generated from the potential earthquake can make up for the inadequate historical information of tsunamis hazard.

There are significant differences in the bottom bathymetry between the South China Sea bordering the

southern province of Guangdong and the East China Sea and Yellow Sea adjacent to the provinces of Zhejiang, Jiangsu, and Shandong. For the two ocean regions, we will compute the probabilities of the tsunami hazard in China Sea area by using both linear and nonlinear models. In the nonlinear model, the Manning roughness is 0.025 for the natural channels in good condition which is suitable for the China Sea.

Due to the prevalence of deep region in South China Sea, the linear model is expected to perform well. Our probability for tsunami wave occurrence is computed from the probability of earthquake occurrence and the probability of maximum wave height of all seismic tsunami induced by potential earthquakes [11]. The tsunami waves with heights of (1.0, 2.0 m) and heights over 2.0 m are considered for hazard evaluation. We consider both economic and scientific factors for wave scales in our tsunami simulation. In our project we only carry out generation and wave propagation of whole tsunami process. Two meters in propagation can be amplified a few times, up to ten times [7, 9], based on local ocean topographical conditions after run-up process computation. Therefore, this wave height size could cause economic hazard after run-up for China coastal area because continental altitude of main Chinese cities only couple meters over the sea. Actually, the wave height of Chinese historical tsunami records is around from half meters to 7.5 m (Keelung, 1867) [16]. Most of Chinese tsunamis are around 1–2 m. We forecast that the probability for tsunami wave with more than 2.0 m to hit within this century is 10.12% for Hong Kong and Macau, 3.40% for Kaohsiung, and 13.34% for Shantou with the linear model. With the nonlinear model, the probability is the same for the same tsunami wave height at Hong Kong and Macau, and Kaohsiung, while a lower probability at Shantou of 10.12% is found. In general, the probabilities for most coastal cities do not change with the usage of nonlinear theory. Both results indicate that tsunami hazard can be induced on Hong Kong coastal area with more than 2.0 m tsunami hazard with around probability of 1% every decade. These results are similar to the same as the frequency of destructive seismic event in South China Sea and adjacent region.

Here, we visualize the time-dependent results from the linear and nonlinear models of the tsunami propagation in eastern China Sea region (Fig. 7). In eastern China Sea area the ocean depth of most part is very shallow, less than 300 m. Comparison of the simulations with data on the evolution of leading wave amplitude across the entire region indicates that there is an appreciable influence from the varying depth. Hence, the nonlinear model must be applied for the eastern China Sea region. For forecasting the potential coastal tsunami hazard in the eastern China Sea region in this century, we have calculated the probability distribution for tsunami wave higher than 2.0 m wave hitting the ocean entrance to Yangtze river, the northeastern coast of Zhejiang province, and northern Taiwan island [12]. There is also have a potential chance for them to be hit by tsunami hazard for 1.0–2.0 m. There are different probabilities for a 2.0 m tsunami wave to hit The major cities along eastern Chinese coast, 0.52% for Shanghai, 3.2% for Wenzhou, and 7.2% for Keelung within the next 100 years. The probability is 7.2% for a 1.0–2.0 m tsunami wave to hit Shanghai [12].

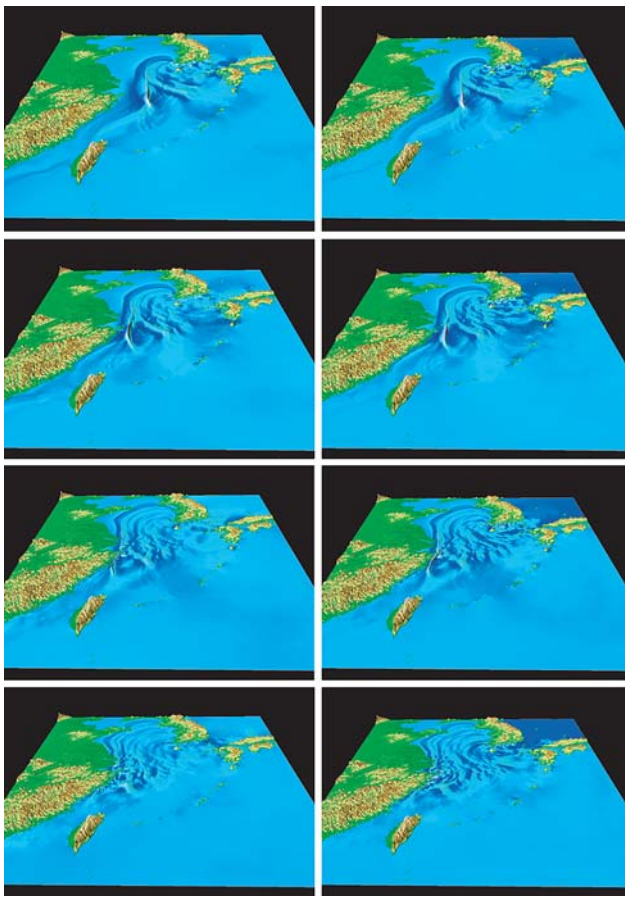

Fig. 7 Visualization of comparison for tsunami wave propagation in linear and nonlinear shallow water models at four different traveling times in eastern China Sea region. *Left* column shows nonlinear model, *right* one shows linear model. The waveforms of two models are almost the same in deep ocean (first wave snapshot). But waveforms in two models are different in shallow ocean part (the rest wave snapshots)

Based on previous analysis, we can predict the potential tsunami hazard with the linear shallow water equation (Eq. 1) in South China Sea with its natural bottom boundary condition due to its bathymetry (Fig. 1). However, we have to employ the nonlinear model (Eq. 2) in the eastern China Sea region, for which the bottom frictional effect must also be considered.

4 Conclusion

We investigated the economic disruption caused by a pair of Taiwan earthquakes on 26 December 2006. A larger earthquake along the Luzon Trench would have much more severe global consequences because of Internet connectivity of the cables at the bottom of the South China Sea, which were damaged by the submarine landslide. We have reacted rapidly by carrying out this comparison of linear and nonlinear predictions of tsunami wave propagation across the South China Sea. From our analysis, we concluded that one can apply linear theory to a good accuracy for this critical region (Manning roughness $n = 0.025$). This would allow a much earlier warning to be issued, since the linear calculations can be carried out on laptops in nearly real time. In addition, we found that the bottom frictional properties of the seafloor due to sediments can play an important role in quenching the magnitude of incipient tsunami waves. The same statement concerning the applicability of the linear theory will not be true for eastern China Sea region. Because of its much shallower seafloor, the nonlinear theory must be carried out in this region.

Acknowledgments We would like to thank Professor Fumihiko Imamura for providing computational codes TUNAMI_N1 and TUNAMI_N2, and his kind guidance on tsunami numerical modeling. This research is supported by National Science Foundation of China (NSFC-40574021, 40728004) and the EAR program of the US National Science Foundation.

References

1. Cho Y-S, Sohna D-H, Lee S (2007) Practical modified scheme of linear shallow-water equations for distant propagation of tsunamis. Ocean Eng V34:1769–1777
2. Comer RP (1984) Tsunami generation: a comparison of traditional and normal mode approaches. Geophys J Int 77(1):29–41
3. Geist EL (1998) Local tsunamis and earthquake source parameters. Adv Geophys 39:116–209
4. George DL, LeVeque RJ (2006) Finite volume methods and adaptive refinement for global tsunami propagation and indundation, Science of Tsunami Hazards, No. 5, V25, pp 319–328
5. Goto C, Ogawa Y, Shuto N, Imamura N (1997) Numerical method of tsunami simulation with the leap-frog scheme (IUGG/IOC Time Project), IOC manual, UNESCO, No. 35
6. Grilli S, Svendsen I, Subramanya R (1997) Breaking criterion and characteristics for solitary waves on slopes. J Waterway Port Coastal Ocean Eng 123(3):102–112
7. Gutenberg B, Richter CF (1949) Seismicity of the Earth and associated phenomena, Princeton University Press, Princeton
8. Kajiura K (1970) Tsunami source, energy and the directivity of wave radiation. Bull Earthquake Res Inst Tokyo Univ 48:835–869
9. Jensen A, Pedersem GK, Wood DJ (2003) An experimental study of wave run-up at a steep beach ATLE. J Fluid Mech 486:61–188
10. Novikova T, Wen K-L, Huang B-S (2000) Amplification of gravity and Rayleigh waves in a layered water–soil model. Earth Planets Space 52:579–586
11. Liu Y, Santos A, Wang SM, Shi Y, Liu H, Yuen DA (2007) Tsunami hazards from potential earthquakes along South China Coast. Phys Earth Planet Inter 163:233–245
12. Liu Y, Shi Y, Sevre EOD, Yuen DA, Xing H (2007) Probabilistic forecast of tsunami hazards along Chinese Coast. Visual Geosciences (Book), Springer, Heidelberg (submitted)
13. Liu Z et al (1988) South China Sea geology tectonic and continental margin extension (in Chinese), Science Press, Beijing
14. Okada Y (1985) Surface deformation due to shear and tensile faults in a half-space. Bull Seism Soc Am 75:1135–1154
15. Reiter L (1990) Earthquake hazard analysis: issues and insights. Columbia University Press, New York
16. Wang F, Zhang Z (2005) Earthquake tsunami record in Chinese ancient books. Chinese Earthquakes 21, V03:437–443
17. Wang J (1996) Global linear stability of the two-dimensional shallow-water equations: an application of the distributive theorem of roots for polynomials on the unit circle. Mon Wea Rev 124:1301–1310
18. Ward S (1982) On tsunami nucleation: an instantaneous modulated line source. Phys Earth Planet Int 27:273–285
19. Wells D, Coppersmith K (1994) New empirical relationships among magnitude, rupture length, rupture area, and surface displacement. Bull Seismol Soc Am 84:974–1002
20. Yamashita T, Sato R (1976) Correlation of tsunami and sub-oceanic Rayleigh wave amplitudes. J Phys Earth 24:397–416
21. Zang S, Ning J (2002) Interaction between Philippine Sea Place (PH) and Eurasia (EU) Plate and its influence on the movment eastern Asia. Chinese Journal of Geophysics, 45, V01:188–197